Chapter 3: A Generalized Nusselt Number Correlation for Nanofluids and Look-up Diagram to Select Heat Transfer Fluids

Considering the literature review and the underlined research gaps, this chapter provides (a) a comparative assessment of the available dimensional parameters using different HTFs, (b) a non-dimensional parameter called *figure of merit* for selecting an HTF, (c) a comparative assessment of the reported Nusselt number correlations for nanofluids (see Table 2.1), and (d) a novel *separation approach* for deducing a generalized Nusselt number correlations for water-based and oil-based nanofluids.

3.1 Selection Criteria for Heat Transfer Fluids

This section discusses the available dimensional criteria and a non-dimensional figure of merit for selecting pure-fluid, nanofluids, or hybrid nanofluids. Furthermore, the required thermophysical properties and the correlation of *Nu* are presented in this section. These are discussed subsequently.

3.1.1 Dimensional and Non-dimensional Parameters

It may be argued that both fluid and flow properties will affect the convective heat transfer process using a fluid. Some important fluid properties are the coefficient of expansion, viscosity, heat capacity, thermal conductivity, freezing point, boiling point, flash point, corrosiveness, and stability. However, the thermophysical properties of a fluid are mainly considered to derive some of the dimensional selection criteria and are summarized in Table 3.1. A high value of thermal conductivity is preferred to promote heat transfer to a fluid, a high value of heat capacity is preferred for volumetric heat storage, and low viscosity is preferred to reduce the required pumping power, see Becker [59]. Mouromtseff used the cooling of vacuum tubes along the radial direction to define the *Mo* number. Mouromtseff

actually deduced convective coefficient for internal turbulent flow based on Dittus-Boelter correlation. For the convective heat transfer along the axial direction, Bonilla expressed *Bo*. Bonilla ignored the heat from the wall. Lenert deduced the expression for a normalized pressure drop to optimize the design of a multi-channel heat sink, as in Murakami and Mikic [60]. Volumetric heat capacity is the dimensional parameter to measure the storage heat capacity. These dimensional numbers and the respective physical interpretation are given in Table 3.1. In addition to these dimensional numbers, a non-dimensional figure of merit (FoM) is included in the present work as a potential selection criterion.

As compared to dimensional parameter, a nondimensional parameter has adavantage that it reduces the number of parameter also, it is independent of dimensions. The objective here is to select the heat transfer fluid for heating/cooling applications. In order to achieve this, the fluid having high heat transfer characteristics and also lower pressure drop should be selected. In the search of nondimensional parameter, Nusselt number (Nu) is selected for heat transfer characteristics of the fluid and coefficient of pressure (CP) is selected to get pressure drop. Both Nusselt number and Coefficient of pressure is non dimensional number. It is obvious that high Nusselt number and lower Coefficient of pressure is required to select a heat transfer fluid. Thus in the figure of merit (Nu/CP), *Nu* number is in numerator and CP is in denominator is selected in such a way that the fluid having higher figure of merit should be selected for further applications. This clearly defines the relative effectiveness of heat transfer concerning the pressure drop in a system. For nanofluid another nondimensional parameter, correction factor (η), is taken to separate the effects of nanoparticles, discussed in section 3.1.3.3.. The results and discussion provide a comparative assessment of these parameters/criteria.

Table 3.1 Dimensional and non-dimensional parameters

Dimensional parameter	Expression	Interpretation/remarks
Mo (Mouromtseff number) [61][62]	$\frac{\rho^{0.8} {c_p}^{0.33} k^{0.67}}{\mu^{0.47}}$	Heat transfer coefficient deduced from the Dittus-Boelter correlation [63].
Bo(Bonilla Number) [61][62]	$\frac{\rho^2 {c_p}^{2.8}}{\mu^{0.2}}$	Represents the inverse of pumping power to maintain a given temperature difference.
Lenert number [62]	$\frac{\rho^2 {c_p}^{1.6} k^{1.8}}{\mu^{1.4}}$	The inverse of the normalized pumping power, considered both radial and axial heat flow
Volumetric heat capacity	ρc_p	The measure of heat storage capacity
Non-dimensional Parameter		
Figure of Merit (FoM)	Pure fluid $\frac{Nu}{\mathrm{CP}}$ Nanofluid/Hybrid-nanofluid $\frac{\eta Nu}{\mathrm{CP}}$	a. Heat transfer relative to pressure drop. A high value of this number is preferred for selecting a heat transfer fluid. b. The correction factor η is to be obtained for incorporating the separate effect of nanoparticles.

Table 3.1 shows that a *Nu* correlation is needed to calculate FoM. For the pure fluids, Incropera and DeWitt [63] reported that uncertainty in Dittus–Boelter's *Nu*

correlation is about 25%, and that of Gnielinski's correlation is about 10%. The required friction factor (*f*) is estimated using equation 3.1. The coefficient of pressure (CP) in FoM is defined as the ratio of pressure drop to dynamic pressure. FoM is calculated assuming a fully developed turbulent flow in a pipe, having a length (L) to diameter (D) ratio of 200. This length is considerably greater than the entrance length of 60D. The calculation for FoM is given as follows:

$$FoM = \frac{Nu}{\mathrm{CP}} \; or \; \frac{\eta Nu}{\mathrm{CP}}, \text{ with } \mathrm{CP} = \frac{\Delta p}{0.5\rho V^2}. \tag{3.1}$$

Where, $\Delta p = \frac{\rho f L V^2}{2D}$ and $f = (1.84 \log Re - 1.64)^{-2}$.

The involved properties for some pure fluid, nanofluids, and hybrid nanofluids are presented in sub-sections 3.1.2 and 3.1.3. Finally, it may be emphasized that a *Nu* correlation is required for nanofluids and hybrid nanofluids to deduce the correction factor η in FoM, which is discussed in sub-section 3.1.3.2.

3.1.2 Pure Fluids

The selected pure fluids based on a literature review in the medium-temperature range of 373-573 K are vegetable oil (Canola and Soybean), Therminol (VP1 and 66), and molten salts (e.g., Hitec, Hitec-XL, and solar salt). The list can be extended; however, the variety serves the current purpose, i.e., the development of systematic analysis-based selection criteria for heat transfer fluid. The composition, thermophysical property correlations, and temperature range of these heat transfer fluids are shown in Table 3.2. It may be underlined that the available correlations for the thermophysical properties of vegetable oil are extended from 423 to 453 K following the linear trend of the same, except for viscosity [11][12]. There are three different models for temperature-dependent viscosity, namely Arrhenius, modified Williams Landley-Ferry (WLF), and power law. The analysis of these

models revealed that the modified WLF offers a comparatively low standard error of estimate or a low relative average deviation.

Table 3.2 Heat transfer fluid (HTF) composition, thermophysical properties, and temperature range.

Fluid-type	HTF and temperature (in K)	Composition	Properties/correlation
Vegetable Oil [11][12]	Canola (CA) 293-453	Miristic (C14:0) 0.061%, Palmitic (C16:0) 4%, Estearic (C18:0) 1.62%, Oleic (C18:1) 58.53%, Linoleic (C18:2) 25.26%, Linolenic (C18:3) 10.20%	$\rho = 990.070 - 0.237T$ $c_p = 287 + 5.3T$ $k = 0.139 + 0.0001T$ $\ln(\mu \times 10^3) = \frac{0.8694T}{-237.4607 + T}$
	Soybean (SB) 293-453	Miristic (C14:0) 0.12%, Palmitic (C16:0) 10.51%, Estearic (C18:0) 3.22%, Oleic (C18:1) 22.31%, Linoleic (C18:2) 53.58%, Linolenic (C18:3) 8.50%	$\rho = 1039.225 - 0.397T$ $c_p = 1024 + 3T$ $k = 0.134 + 0.0001T$ $\ln(\mu \times 10^3) = \frac{0.7442T}{-240.4647 + T}$

Thermal oil [2]	TherminolVP 1 (TVP1) 285-673	Eutectic mixture of Dipehyloxide (73.5%) and Diphenyl (26.5%)	Engineering Equation Solver Library [97]
	Therminol66 (T66) 283-644	Hydrogenated terphenyl	
Molten salt [2]	Solar salt (SS) 533- 873	A binary mixture of $NaNO_3$ (60%)-KNO_3 (40%)	$\rho = 2090 - 0.636(T - 273.15)$ $c_p = 1443 - 0.172(T - 273.15)$ $k = 0.443 + 1.9 \times 10^{-4}(T - 273.15)$ $\mu = 2.2714 \times 10^{-2} - 1.2 \times 10^{-4}(T - 273.15) + 2.281 \times 10^{-7}(T - 273.15)^2 - 1.474 \times 10^{-10}(T - 273.15)^3$
	Hitec (H) 415-808	Ternary Mixture of alkali nitrate or nitride $NaNO_3$ (7%)-KNO_3 (53%) -$NaNO_2$ (40)	$\rho = -0.74(T - 273.15) + 2084$ $c_p = 1560$ $k = 0.411 + 4.36 \times 10^{-4}(T - 273.15) - 1.54 \times 10^{-6}(T - 273.15)^2$ $\mu = 10^{2.737}(T - 273.15)^{-2.104}$
	Hitec XL (HXL) 403-823	Ternary Nitrate mixture of $NaNO_3$ (7%) KNO_3 (45%)-$Ca(NO_3)_2$ (48%)	$\rho = 2240 - 0.827(T - 273.15)$ $c_p = -0.33T + 1634$ $k = 0.519$ $\mu = 10^{6.137}(\mathrm{T} - 273.15)^{-3.364}$
	Nano fluid	NF	$\phi = \frac{1}{(\frac{100}{\phi_m}\frac{\rho_p}{\rho_{BF}} + 1)} 100\%$ $\rho_{NF} = (1 - \phi)\rho_{BF} + \phi\rho_P$

Nanofluid (NP-BF) [98][99][100]			$c_{PNF} = \frac{(1-\phi)\rho_{BF}c_{PBF} + \phi\rho_P c_{P,P}}{\rho_{NF}}$ $c_{PNF} = \frac{\phi_s\rho_s c_{Ps} + \phi_{np}\rho_{np}c_{P,np} + \phi_{ns}\rho_{ns}c_{P,ns}}{\phi_s\rho_s + \phi_{np}\rho_{np} + \phi_{ns}\rho_{ns}}$ $k_{NF} = \frac{k_P+(n-1)k_{BF}-((n-1)\phi(k_{BF}-k_P))}{k_P+(n-1)k_{BF}+\phi(k_{BF}-k_P)}k_{BF}$ $\mu_{NF} = \mu_{BF}(1 + A_1\phi + A_2\phi^2)$
Hybrid-nanofluid (NP_1-NP_2-BF) [101]	Hybrid-nanofluid	NP_1-NP_2-BF	$\rho_{HNF} = (1-\phi_1-\phi_2)\rho_{BF} + \phi_1\rho_{P1} + \phi_2\rho_{P2}$ $c_{P,HNF}\rho_{HNF} = (1-\phi_1-\phi_2)\rho_{BF}c_{P,BF} + \phi_1\rho_{P1}c_{P,P1} + \phi_2\rho_{P2}c_{P,P2}$ $k_{HNF} = \frac{k_{NF1}\phi_1 + k_{NF2}\phi_2}{\phi}$ $\mu_{HNF} = \frac{\mu_{NF1}\phi_1 + \mu_{NF2}\phi_2}{\phi}$

3.1.3 Nanofluids

3.1.3.1 Thermophysical Properties

The selection of nanofluids is based on availability, which is mostly water-based. However, due care is taken while selecting the nanoparticles, including oxides, metals, CNT, and graphene, for broader consideration. The common thermophysical properties of the nanofluids, which influence heat transfer, are density, specific heat capacity, viscosity, and thermal conductivity, and their correlations used in this investigation are given in Table 3.2. It may be noted that two different models (thermal equilibrium model [98] and nanolayer-based model [99]) available in the literature for nanofluid-specific heat are given in the table. Literature suggests it's a decreasing and increasing trend for nanofluids [56][102][103][104]. For example, experiments reported decreasing values of c_p for (a) Al_2O_3, TiO_2 and Al nanoparticle in deionised water (W), ethylene glycol (EG) and engine

oil [105], (b) Al_2O_3-EG/W (60:40), ZnO-EG/W (60:40) and SiO_2-water nanofluid [106], Titania –Therminol55 nanofluids [107] , (c) SiO_2- EG, glycerol nanofluids [108] and (d) functionalized Al_2O_3-Thermal oil [109], 16% enhancement of c_p for 2% copper – gear-oil nanofluid [110], and significant enhancement in c_p for several nanosalts [56][103][104]. The conditional enhancement for c_p of nanosalt was explained with e.g. chain-like structure [102] and mesolayer based models [111]. Moreover, the literature review revealed the predictive capability of the widely used expression of c_p, in Table 3.2, for water or some oil-based nanofluids. There is no certain rule to represent the c_p for all nanofluids. As in the present study, the experimental data of various water-based nanoparticles dispersed nanofluids are taken from various literature, which are used to develop the proposed Nusselt number correlations, and hence, the thermal equilibrium model has been used. This model does not explain the increasing nature of c_p due to the internal and nanoscopic organization of the nanofluid, which is a limitation of this model. There are no well-accepted correlations for viscosity and thermal conductivity. There are some theoretical models, mostly for microfluids and with spherical-shaped particles. These are not validated with the nanofluid-specific experimental data and empirical correlations. In general, viscosity and thermal conductivity of nanofluids depend on individual properties, nanoparticle shape and size; however, no such correlations are available. The significant effect of nanoparticle shape on the transport properties is shown. Hence, the effect of nanoparticle size is neglected considering (a) the negligible variation of properties, within an acceptable size range, and (b) that it is practically not possible to synthesize the same size of nanoparticles. However, the shape-dependent correlations are adopted in Table 3.2 for this study.

Table 3.3 Parameters to define the shapes of nanoparticles [100]

Shape / Parameter	Spherical	Brick	Cylinder	Platelet
Sphericity(ψ)	1	0.81	0.62	0.52
Shape factor $n=3/\psi$	3	3.7	4.9	5.7
A_1	2.5	1.9	13.5	37.1
A_2	6.2	471.4	904.4	612.6

The parameters describing the different nanoparticle shapes (spherical, brick, cylindrical, and platelet), i.e., sphericity *(ψ),* shape factor *(n),* constant A_1, A_2, and their values, are summarized in Table 3.3. These are utilized to calculate the thermophysical properties of nanofluids using the suggested formulations in Table 3.2 for density, specific heat capacity, thermal conductivity, and absolute viscosity. One challenge while selecting these properties is that the base fluid is water; thus, the operating temperature of the selected water-based nanofluids is less than 373 K. The thermophysical properties of selected nanoparticles are summarized in Table 3.4. The constant values assume a limited variation in these properties within a narrow temperature range below 373 K. The variations in reported values of thermophysical properties of nanoparticles are quite significant, especially for graphene. Nonetheless, efforts are being made to collect the available data, ensuring their reliability from the referred literature. Therefore, the temperature-dependent base fluid properties are generally used to evaluate the nanofluid properties in 373-573 K to address the property variation with temperature.

Table 3.4 Thermophysical properties of nanoparticles.

Nanoparticles → Properties ↓	γAl_2O_3	Copper Oxide (CuO)	Copper (Cu)	Carbon Nanotube (CNT)	Graphene	Titanium Oxide (TiO_2)	MgO [71]
Density ρ_p(kg/m^3)	3970 [101] 3700 [112]	6350 [113] 6500 [67]	8933 [101]	2100 [101]	2200 [101] 1100 [114]	4250 [101] 4175 [115]	3580 [70]
Specific heat c_p(J/kg K)	765 [101] 880 [112]	535.6 [113] 533 [67]	385 [101]	410 [101]	790 [101] 710 [114]	692.0 [115] 686.2 [101]	961 [70]
Thermal conductivity k_p (W/mK)	46 [112] 40 [101]	69 [113] 17.65 [67]	400 [101]	3007.4 [101]	3000 [114] 5000 [101]	8.40 [115] 8.95 [101]	41 [70]
Thermal diffusivity α_p (x10^{7}m^2/s)	131.7 [101]	57.4 [101]	1163 [101]	34929.1 [101]	28768.7 [101]	30.7 [101]	119.2 [70]

3.1.3.2 Nusselt Number Correlation

It is realized that *Nu* correlations are required for pure fluids and nanofluids to calculate FoM. The selection of Gnielinski's *Nu* correlation for pure or base fluid is straightforward (see Table 2.1). It is worthwhile to note that this correlation is valid for a high *Re* and a

wide range of Pr, including vegetable oil and Therminol. Hence, the selection is beneficial even for the nanofluids in which a suitable base fluid is to be selected in 373-573 K. To address this issue, some of the suggested correlations for *Nu* are being reviewed and analyzed. Finally, an approach is proposed to deduce a generalized *Nu* correlation in which a nanofluid is viewed as a combination of nanoparticles and the base fluid. A list of suggested *Nu* correlations for pure fluid, nanofluids, and hybrid nanofluids are provided in Table 2.1. These show that the *Nu* correlation for nanofluids (henceforth represented with Nu_{NF}) is a function of particle shape, particle size, volumetric concentration (ϕ), Reynolds number of nanofluid flow (Re_{NF}), and Prandtl number of nanofluids (Pr_{NF}).

The selection of Nu_{NF} and Nu_{HNF} correlations consider (a) power-law type expressions, (b) their chronological development, (c) different nanoparticles, and (d) applicability for turbulent flow with $10000<Re_{NF}<30000$, as far as possible. The correlations are summarized in Table 2.1. The turbulent flow regime is preferred for concentrated solar thermal system-based heating and cooling applications, see Figure 1.1. The notable difference between Nu_{NF}correlation for nanofluid and Nu_{HNF} correlation for hybrid nanofluids is the exponent of ϕ (see Table 2.2), possibly, depicting the effect of nanoparticle-nanoparticle interaction. Thus, it may be safely stated that the effect of the flow regime on Nu_{HNF} will remain practically the same, for a base fluid and small values of ϕ. In other words, using these limited resources, the findings for nanofluids are adopted for hybrid nanofluids, as of now. These are generally obtained for a temperature < 373 K with water as the base fluid and mostly oxides as nanoparticles. However, the selected medium-temperature in 373-573 K requires heat transfer fluids such as Therminol VP1/66 and vegetable oils. Hence, a strategy is required for adopting such a correlation in the present case.

As the first step, a preliminary analysis is performed to identify a suitable correlation for Nu_{NF} out of the widely available options. A comparison between Nu_{NF} correlations for spherical (CuO) and cylindrical (CNT) shaped nanoparticle dispersed nanofluids, with water as a base fluid, is shown in Figure 3.1. This reveals that Nu_{NF} correlations from Maiga et al. [65], Sajadi & Kazemi [68], Xuan & Li [64], Sunder et al. [69], Esfe [70], and Minea [57] predict, mostly, within ± 20% for CuO as a nanoparticle. This uncertainty range is adopted in the subsequent analysis. A much higher uncertainty of these correlations is found for CNT-water nanofluid. This is expected as the correlations are mostly deduced with experiments and numerical simulations involving the oxides as nanoparticles. Interestingly, Sajadi & Kazemi [68] correlation shows a better predictive capability for CNT-water nanofluid, which is developed for TiO_2 and valid for a temperature <373 K. However, this observation leaves an indication that a generalized form of Nu_{NF} correlation in the form of power-law is feasible, lending support for selecting the correlations. Therefore, this work is an attempt to extend the applicability of the Nu_{NF} correlation to a wide range of nanoparticles and base fluid. This is necessary for the estimation of FoM to compare the performance of different heat transfer fluids. The two different approaches are worked out. The first approach is including the *separate effect of nanoparticles* in a widely-accepted *Nu* correlation, such as Gnielinski [63] that accounts for a wide range of base fluid in a solution. This methodology is very similar to defining the thermophysical properties of a nanofluid, such as viscosity [100], in which the corresponding parameter of a base fluid is corrected by a factor for the effect of nanoparticle, see Table 3.2. The second approach is the deduction of a correlation based on dedicated experiments. In the subsequent discussion, the first approach is explored. The second approach is underlined for future investigation and is beyond the scope of this work.

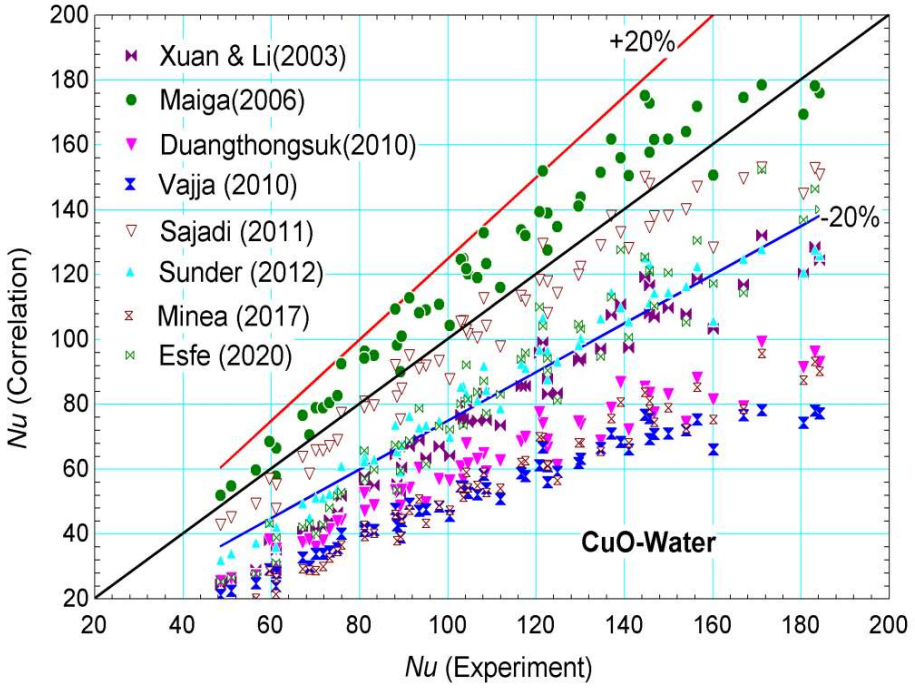

(a)

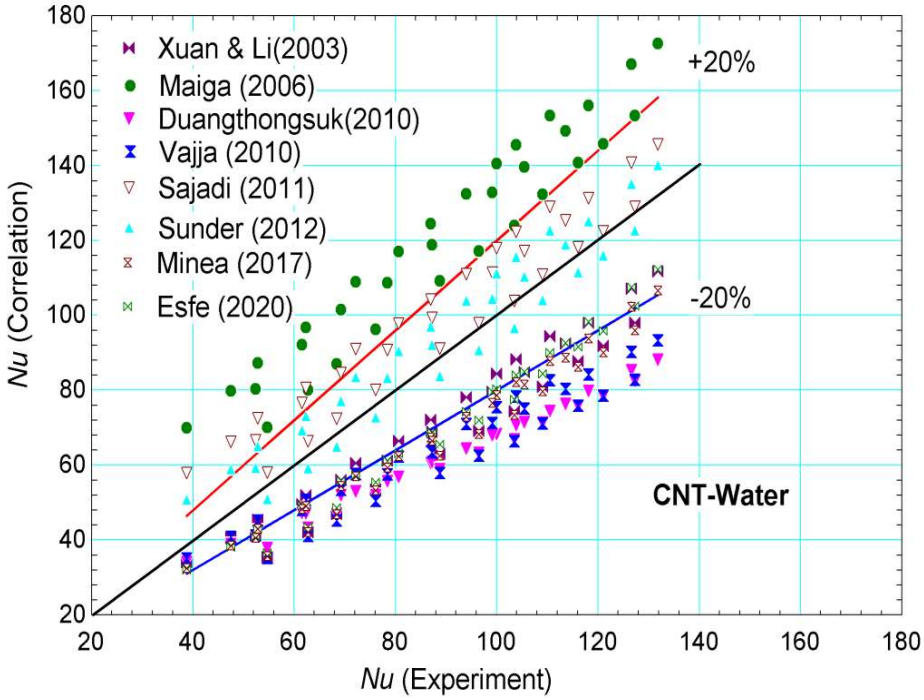

b)

Figure 3.1 A comparison between Nu_{NF} correlations for nanofluids with (a) spherical (CuO) (b) cylindrical (CNT) shaped nanoparticles with water as the base fluid.

3.1.3.3 A Generalized Nusselt Number Correlation: Separation Approach

This section proposes an approach for including the separate effect of nanoparticles in a Nu correlation for base fluid. This is based on the assumption that (a) nanofluids comprise base fluid with uniformly dispersed nanoparticles, and (b) interactions between nanoparticles do not alter the bulk fluid flow regime due to a negligible concentration, which excludes the transition from laminar to turbulent flow regime. Accordingly, the separate effects of nanoparticles and base fluid are combined to form Nu_{NF}. The simplest possible *separation approach* to obtain a correlation for Nu_{NF} is illustrated as a flowchart in Figure 3.2. Step 1 identifies all the non-dimensional parameters describing the fluid flow regime, fluid property, and nanoparticles. Step 2 separates the effect of base fluid flow and the effect of suspended nanoparticles. Finally, Nu_{NF} is represented as a product of η and Nu_{BF} in equation 3.2, where η is the correction factor to account for the effect of the nanoparticle.

$$\underbrace{Nu_{NF}}_{\substack{\text{to be selected for}\\ \text{nanofluids from literature}\\ (\textbf{which correlation}??)}} = \underbrace{\eta}_{\substack{\text{for the separate effect}\\ \text{of nanoparticles}\\ (\textbf{unknown correction factor})}} \underbrace{Nu_{BF}}_{\substack{\text{selected to account}\\ \text{for base-fluid flow}\\ (\text{known},\textbf{Gnielinski})}} \tag{3.2}$$

where $\eta = C_1 \alpha_r^{C_2} \phi^{C_3} n^{C_4}$.

Equation 3.2 filters the effect of nanoparticles and contains two unknowns Nu_{NF} and η. Therefore, equation 3.2 is not closed. For the second term in RHS (Nu_{BF}) Gnielinski correlation is selected to describe the effect of base fluid flow. Here, the subscript BF stands for base fluid. Hereinafter, the symbol Nu_{BF} is utilized to avoid any confusion with pure fluid, for which this terminology is redundant. In equation 3.2, the power law is assumed to estimate η. Here, $\alpha_r = \frac{\alpha_p}{\alpha_{BF}}$ is the nanoparticle and base fluid thermal diffusivity ratio, and C_1 to C_4 are the unknown coefficients to be estimated.

Assuming the known Nu_{NF} and Nu_{BF} in equation 3.2, the developed regression analysis for estimating coefficients C_1 to C_4 in η, is described henceforth. The equation 3.2. can be re-written as follows:

$$\frac{Nu_{NF}}{Nu_{BF}} = C_1 \alpha_r^{C_2} \phi^{C_3} n^{C_4}. \tag{3.3}$$

Taking *log* on both sides leads to,

$$\log \frac{Nu_{NF}}{Nu_{BF}} = \log C_1 + C_2 \log \alpha_r + C_3 \log \phi + C_4 \log n. \tag{3.4}$$

Let, $Q = \log \frac{Nu_{NF}}{Nu_{BF}}$, $C = \log C_1$, $X = \log \alpha_r$, $Y = \log \phi$, and $Z = \log n$, gives

$$Q = C + C_2 X + C_3 Y + C_4 Z \tag{3.5}$$

Let us define E as the measure of error for the estimation of Q as follows:

$$E = \sum_{j=1}^{m} (Q_j - C - C_2 X_j - C_3 Y_j - C_4 Z_j)^2 \tag{3.6}$$

where m is the sample size. To minimize the error $\frac{\partial E}{\partial C} = 0$, and $\frac{\partial E}{\partial C_k} = 0$, for $k = 2,3,4$. The subsequent simplification gives,

$$\begin{pmatrix} m & \sum X_j & \sum Y_j & \sum Z_j \\ \sum X_j & \sum X_j^2 & \sum X_j Y_j & \sum X_j Z_j \\ \sum Y_j & \sum Y_j X_j & \sum Y_j^2 & \sum Y_j Z_j \\ \sum Z_j & \sum Z_j X_j & \sum Z_j Y_j & \sum Z_j^2 \end{pmatrix} \begin{pmatrix} C \\ C_2 \\ C_3 \\ C_4 \end{pmatrix} = \begin{pmatrix} \sum Q_j \\ \sum X_j Q_j \\ \sum Y_j Q_j \\ \sum Z_j Q_j \end{pmatrix} \tag{3.7}$$

$for\ j = 1 \ldots m$

Solving the linear system in equation 3.7 gives $C\ (logC_1)$, C_2, $C_3, and\ C_4$, which describes the separate effect of nanoparticles. The calculated values are provided in section 3.2. The final form of separation-based generalized Nusselt number correlation for hybrid nanofluids will be as follows:

$$Nu_{NF} = \underbrace{C_1 \alpha_r^{C_2} \phi^{C_3} n^{C_4}}_{known} \quad \underbrace{Nu_{BF}}_{\text{(known, Gnielinski)}} \tag{3.8}$$

As an extension, the Nusselt number correlation for hybrid nanofluids may be expressed as $Nu_{HNF} = \eta Nu_{BF}$, where $\eta = \eta_1 \eta_2 .. \eta_i \ldots \eta_k$, for k number of nanoparticles based hybrid nanofluids, and η_i is the correction factor for i^{th} nanoparticle. This will be attempted in the future with a comprehensive database for two or three nanoparticle-based hybrid nanofluids. The following expression is used for estimating the effective thermal diffusivity for two nanoparticles-based hybrid nanofluids:

$\alpha_p = \frac{\phi_1 \alpha_{p1} + \phi_2 \alpha_{p2}}{\phi}$, where $n = \frac{\phi_1 n_1 + \phi_2 n_2}{\phi}$ and $\phi = \phi_1 + \phi_2$.

This simple approach benefits from the fact that (a) the thermophysical properties of nanoparticles are enough to estimate η, and (b) the Gnielinski correlation is applicable for 0.5<*Pr*<2000 that includes vegetable oil, TherminolVP1/66, and (c) the dependence of Nu_{NF} on the thermophysical property correlations for nanofluids is mitigated. Therefore, equation 3.2 is regarded as a generalized form of Nu_{NF} correlation. There is a dearth of experiment-based *Nu* correlation for nanosalts, which is necessary to estimate η, and validate the correlation for 10000 <*Re* < 25000 [56][103]. However, the separation approach remains independent of the same. Thus, in the future, an attempt will be made to assess the generalized form of Nu_{NF} correlation for nanosalts.

The benefits of this separation approach is that it filters out the effect of nanoparticles from the nanofluid, only particles thermophysical properties is needed and directly one can get the *Nu* of nanofluid. The obtained generalized correlation is valid for turbulent flow and also valid for wider range of fluid. The limitation of this approach is that while separately considering effect of nanofluids and base fluid, might not sure all the phenomenon is incorporated in this. It is assumed that the nanoparticle does not alter the

flow field (or negligible). It may be true for lower concentration. How can a nanoscale alter the microscale phenomena? So this is the limitations of the separation approach. To incorporate all phenomenon more experiments are required to be performed.

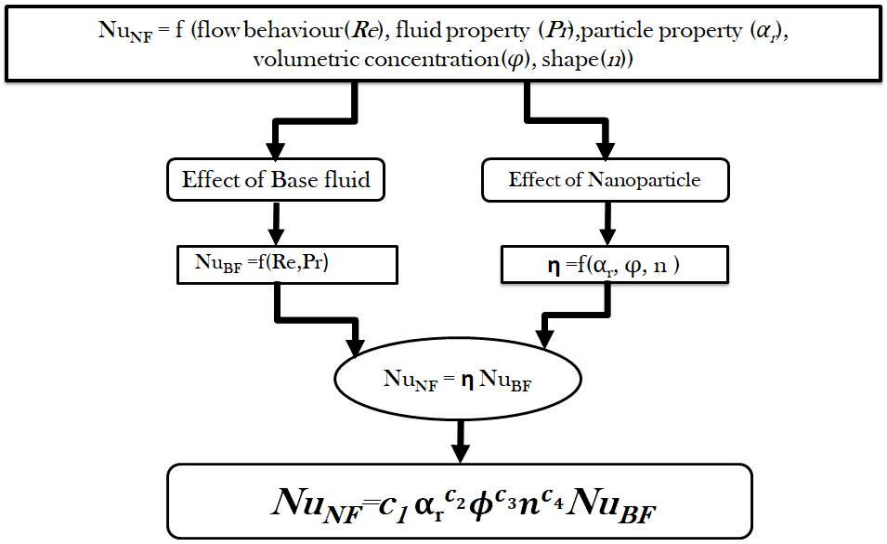

Figure 3.2 A separation approach to obtain Nu_{NF} for nanofluids using Nu_{BF} for base fluid and the correction factor (η) for nanoparticles.

The analysis of Figure 3.1 concludes the need to develop a generalized form of Nu_{NF}. The same is attempted, using some of the reported experimental data from the literature, as summarized in Table 3.5. The selected nanoparticle includes oxides, metal, CNT, and graphene, having different shapes and a wide variation in the thermophysical properties. As the next step, the widely preferred power-law approach is used to derive a correlation, i.e., $Nu_{NF} = CRe_{NF}{}^{m}Pr_{NF}{}^{n}$. The coefficient C and the exponents (m, n) are obtained using an available data analysis tool from MS-Excel. More than three hundred experiments based data for Nu_{NF} are collected from the reported literature, as summarized in Table 3.5. Almost half of these experimental data are utilized for deducing Nu_{NF}, with an expectation that this correlation applies to a wide range of nanoparticle types and their

shapes. The rest of the data is utilized to test the obtained correlation. This is presented in the results and discussion. It is worth mentioning that water is used as the base fluid in all these experiments. Thus, the effect of nanoparticles may be filtered, and therefore, it is expected that the obtained η using this approach will apply to a wide range of nanoparticle types and shapes, as envisaged.

Table 3.5 The collected experimental data for Nu_{NF} with different nanoparticle types, shapes and concentrations.

Nanofluid (particle concentration: *($\boldsymbol{\phi}$ (%))*	Thermophysical property			Re	Uncertainty in Nu	Reference
	ρ_p (kg/m^3)	c_p (J/kg K)	k_p (W/mK)			
γAl_2O_3-water (0.03-0 .135 %)	3700	880	46	4000-30000	4%	[112]
CuO-water (0.015-0.236 %)	6360	535.6	69	4000-25000	4%	[113]
Cu-water (0.3-2 %)	8933	385	401	10000-25000	4%	[64]
TiO_2-water (0.2-2 %)	4175	692	8.4	3000-18000	5%	[66]
Carbon Nanotube (CNT)-water (0.0142-0.095 %)	2100	410	3007	6000-19000	8%	[116]

Graphene Nanoplatelet (GNP)-water (0.0113-0.0453 %)	2220	790	3000	5250-19000	8%	[114]
MgO-water (0.5-2 %)	3580	961	41	6000-32000	14.3%	[70]

3.2 Results and Discussion

This section aims at a comparative assessment of the presented dimensional parameters and non-dimensional FoM. The envisaged outcome is the selection of heat transfer fluid for the discussed solar heating-cooling applications in 373-573 K. This includes a discussion of the improved Nu_{NF} for nanofluids to account for various nanoparticle types and their shapes. This is subsequently presented.

3.2.1 Improved Nusselt Number Correlation for Nanofluids

Using the experimental data and its subsequent analysis leads to the following correlation:

$$Nu_{NF} = 0.074 {Re_{NF}}^{0.72} {Pr_{NF}}^{0.22} \ \ with \ 10000 < Re_{NF} < 25000. \qquad (3.9)$$

A preliminary assessment of this correlation concerning experimental data suggests a $R^2 \sim$ 0.95 with Cu and CuO. A comparative assessment of the proposed correlation in equation 3.3 with Maiga, Xuan & Li, Duangthongsuk, Sajadi & Kazemi, Esfe, Sunder, and Minea, is presented in Figure 3.3. Here, two distinctly different nanoparticles are selected, i.e., CuO and CNT having different thermophysical properties, shapes, and concentrations. Out of these two particles, CuO is widely utilized, whereas CNT is being explored with superior

thermal conductivity. An uncertainty limit of ±20% is utilized for the subsequent analysis and the following are inferred:

a. The Nu_{NF} correlation in equation 3.3 provides a comparable prediction with Sajadi & Kazemi and certainly outperforms Maiga and Xuan & Li correlations for CuO-water and CNT-water nanofluids.

b. Differences between predicted and experimental values of Nu_{NF} are generally higher for CNT-water nanofluid in comparison to CuO-water nanofluid. However, the proposed Nu_{NF} correlation predicts the experimental values, mostly within ±10%, showing an improvement.

Because of the above, further assessment of the proposed correlation for Nu_{NF}, as in equation 3.9, is performed with nanoparticles of different types, shapes, and concentrations. This is required to estimate η for a wide range of nanoparticles.

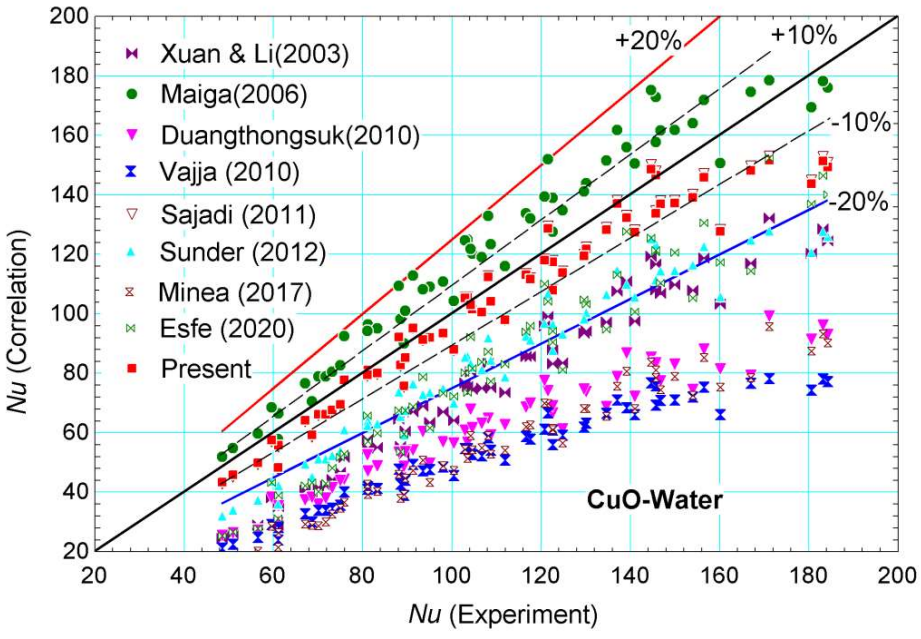

(a)

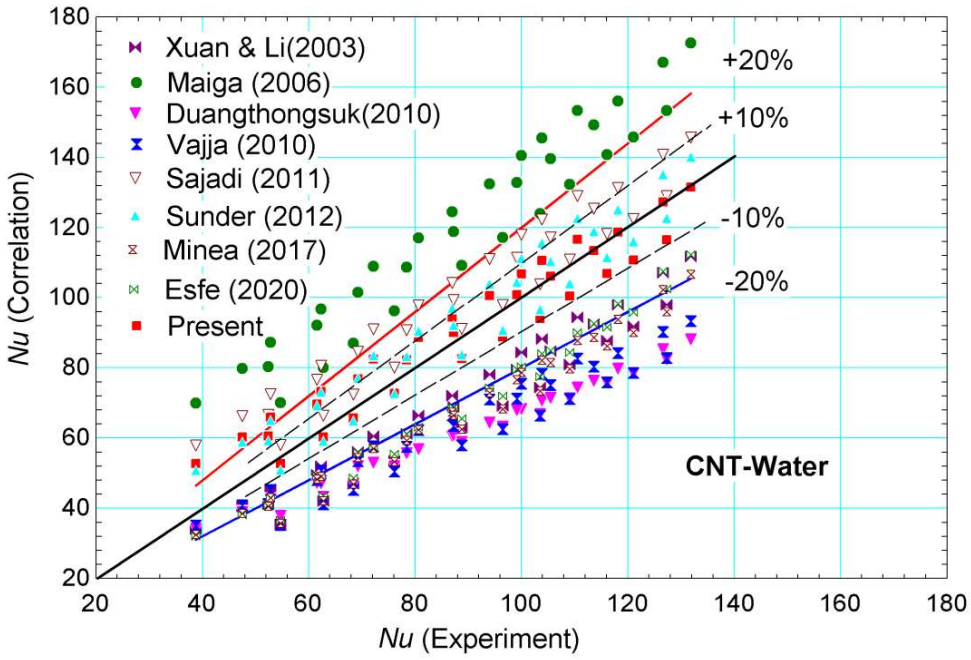

(b)

Figure 3.3 A comparison between correlation in equation 3.9 and experiment-based Nu_{NF} for (a) CuO-water ($\boldsymbol{\phi}$= 0.015 - 0.236 %),and (b) CNT-water ($\boldsymbol{\phi}$=0.0236-0.095 %) nanofluids.

An assessment of the deduced correlation for Nu_{NF} is performed with the remaining experimental data for Cu-water, CuO-water, TiO_2-water, CNT-water, GNP-water, and MgO-water nanofluids with different concentrations of suspended nanoparticles as summarized in Table 3.5. In general, the deduced correlation predicts the measured values of Nu_{NF}, having an uncertainty of about ±20%, except for GNT-water, in which a larger deviation between correlation and experimental values of Nu_{NF} is observed (see Figure 3.4). This may be attributed, to some extent, to the known uncertainty in the properties of GNP. Based on these investigations, it is concluded that (a) the deduced correlation for $Nu_{NF,}$ as in equation 3.9, is capable of predicting the experiment with better accuracy in comparison to other correlations, (b) the correlation is applicable for metals, oxides, CNT and Graphene with a reservation, and (c) possibility of further improvement is foreseen. In this entire

analysis, water is preserved as the base fluid. The calculated R^2 value for Nu_{NF} correlations with the entire dataset are about 0.86 for the present and Sajadi & Kazemi, 0.54 for Maiga, and 0.36 for Xuan & Li. Therefore, in line with our separation approach, the correlation as in equation 3.9 is selected for the estimation of correction factor η with Gnielinski correlation (Nu_{BF}) for base fluid.

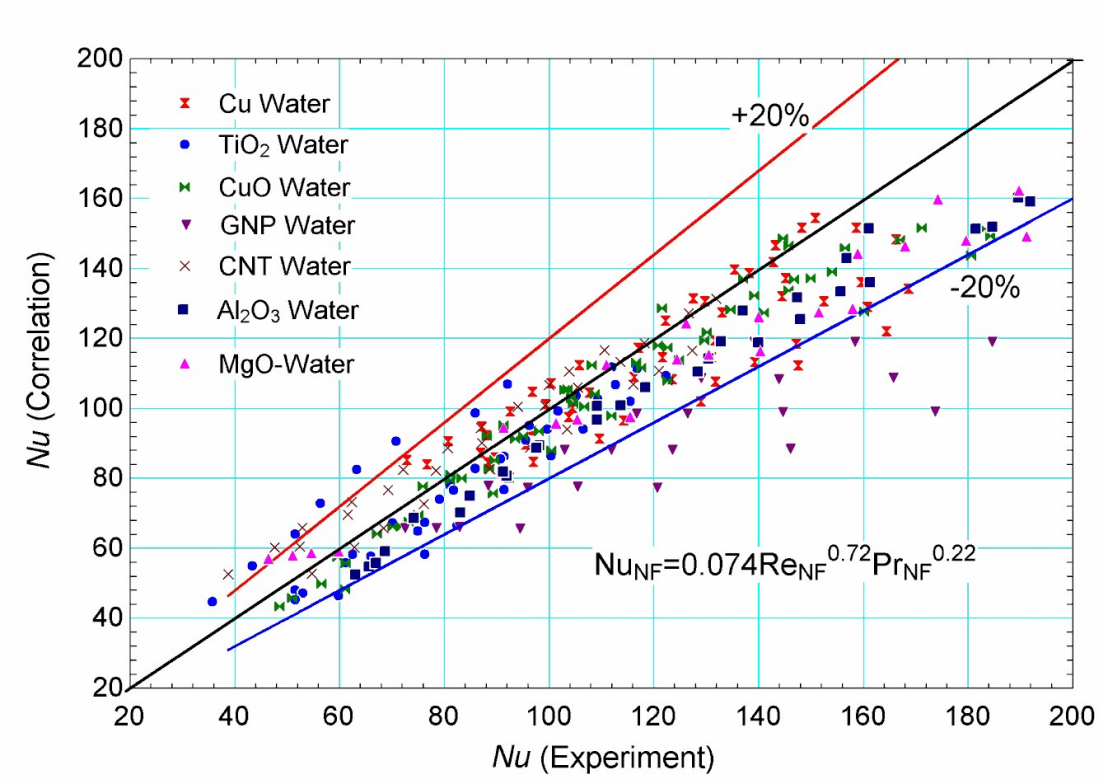

Figure 3.4 A comparison between correlation and experimental Nu_{NF} with different Cu-water, CuO-water, TiO_2-water, CNT-water, GNP-water, Al_2O_3-water, and MgO-water nanofluids. Refer to Table 3.5 for their properties.

.

As discussed, the LHS of equation 3.2 is now available for the estimation of η, which depends on α_r, ϕ and n. Their values are summarized in Table 3.3 and Table 3.4. The estimated values of coefficients C_1 to C_4, with Dittus-Boelter and Gnielnski correlations for Nu_{BF}, are summarized in Table 3.6 to provide flexibility. The values seem

to be consistent, either positive or negative, and the differences are about 10 %. However, continuing our discussion, the Gnielinski correlation for $\boldsymbol{Nu_{BF}}$ is selected.

Table 3.6 Estimated coefficients C_1 to C_4 using Dittus-Boelter and Gnielinski correlations for $Nu_{BF.}$

Parameters →	C_1	C_2	C_3	C_4	Nu_{BF}
Proposed	1.01	-0.062	-0.020	0.346	Dittus-Boelter
values	0.93	-0.059	-0.026	0.357	Gnielinski

Finally, the following expression for Nu_{NF} is recommended:

$$\underbrace{Nu_{NF}}_{\substack{experimentbased\\ inequation\ (3.3)}} = \underbrace{0.93\alpha_r{}^{-0.059}\phi^{-0.026}n^{0.357}}_{\eta} \underbrace{\left\{\frac{\frac{f}{8}(Re-1000)Pr}{1+12.7\sqrt{\frac{f}{8}}\left(Pr^{\frac{2}{3}}-1\right)}\right\}}_{\textbf{Gnielinski correlation, } Nu_{BF}} \tag{3.10}$$

In equation 3.10, the filtered effect of nanoparticles is represented by the correction factor (η).The exponent indicates that η depends strongly on the shape factor (n), and weakly on the volume concentration of nanoparticles (ϕ). The value of α_r is quite high, and thus its dependence is noteworthy. The expression for Nu_{NF}, in terms of the correction factor η, benefits from the fact that (a) Gnielinski correlation for Nu_{BF} is applicable for a wide range of Pr that includes thermal oil, (b) dissimilar to the available nanofluid correlations and is not nanofluid specific, and (c) only the thermophysical properties of nanoparticles are needed. In other words, this correlation is now adaptable to thermal oil-based nanofluids, which is an advantage. The expression for friction factor (f) is given in Table 2.1. This Nu_{NF} correlation is developed based on experiments up to 100 °C; however, it can be adopted for a higher temperature, using the temperature-dependent base fluid properties, as the volume concentration of nanoparticles is generally very low. Thus, the

developed correlation in equation 3.10 may now be termed *generalized* to some extent. A comparison between this correlation and the experiment-based Nu_{NF} reconfirms the previous findings, which is expected. This correlation is used for calculating FoM, which is required for a comparative assessment of the heat transfer fluids. This is discussed subsequently.

3.2.2 Heat Transfer Fluid Selection: Dimensional Parameter

The dimensional parameters in Table 3.1 are analyzed using the thermophysical properties of the selected fluids (Table 3.2). High values of these dimensional parameters are preferred for selecting a heat transfer fluid. Therefore, a temperature-dependent comparative analysis is provided in Table 3.7, which includes an *order of preference* corresponding to a parameter. It may be inferred from Table 3.7 that even for a particular number, like *Mo*, the order of preference changes with temperature. The changes in the order of preference are marked in bold and italics. Also, the different temperature ranges of selected fluids are reflected. An analysis of *Mo,* for instance*,* shows that Cu-TVP1 nanofluid is preferred until 453K, and SS is preferred beyond 533K over all the other fluids. However, the same is not true for *Bo* and other numbers. The analysis using *Mo* and Lenert numbers shows a similar trend up to a certain temperature, which is not true for a temperature exceeding 473K. It may be concluded that the selected nanofluid has a higher preference order based on some dimensional parameters. The prevailing analysis clearly shows an inconsistency between the different dimensional parameters. Therefore, expecting the existence of a *unique selection criterion* is rather a curiosity.

Table 3.7 Analysis of dimensional parameters as in Table 3.1.

Parameter	Temperature (K)	Order of preference

Mo	T=373	CuO-TVP1>TVP1>T66>SB>CA
	T=453	CuO-TVP1>TVP1>H>T66>HXL>SB>CA
	T=473	CuO-TVP1>H>TVP1>HXL>T66
	T=533	SS>H>**CuO-TVP1**>TVP1>HXL>T66
	T=573	SS>H>***HXL***>CuO-TVP1>TVP1>T66
Bo	T=373	TVP1>CuO-TVP1>***CA***>SB>T66
	T=453	***CA***> H> TVP1>CuO-TVP1>***T66***>HXL>SB
	T=473	H>TVP1>CuO-TVP1>T66>HXL
	T=533	***T66***>H>TVP1>*CuO-TVP1*>SS>HXL
	T=573	T66>***TVP1***>H>**CuO-TVP1**>SS>HXL
Lenert number	T=373	CuO-TVP1>TVP1>T66>***SB***>CA
	T=453	CuO-TVP1>TVP1>H>T66>HXL>SB>CA
	T=473	CuO-TVP1>TVP1>H>T66>HXL
	T=533	CuO-TVP1>TVP1>SS>H>T66>HXL
	T=573	***SS***>CuO-TVP1>TVP1>H>***HXL***>T66
ρc_p	T=373	***CA***>SB>CuO-TVP1>TVP1>T66
	T=453	HXL>H>CA>SB>***T66***>CuO-TVP1>TVP1
	T=473	HXL>H>T66>CuO-TVP1>TVP1
	T=533	HXL>H>SS>T66>CuO-TVP1>TVP1
	T=573	***H***>HXL>SS>T66>CuO-TVP1>TVP1

Now, it is realized that using the dimensional number will lead to a subjective conclusion depending on the operating conditions and geometry of the problem. To address this aspect, the non-dimensional figure of merit (FoM) is included in Table 3.1. A high value of this number will be preferred for selecting a heat transfer fluid, primarily aiming

at heat removal from the solar field and its transport to thermal energy storage. The analysis of FoM for different oils and some nanofluids is presented subsequently. The operating ranges of these fluids are summarized in Table 3.2. The deduced equation 3.4 will now be utilized to assess FoM with nanofluids. For consistency, the Gnielinski correlation is selected for pure fluids, as already explained.

3.2.3 Heat Transfer Fluid Selection: Non-dimensional Figure of Merit

The non-dimensional FoM (Nu/CP) is analyzed in this sub-section with different pure fluids and nanofluids. A comparative assessment of FoM with these fluids in the 373-573 K temperature range is presented in Figure 3.5 at 453K and 573K. The selection of these conditions is motivated by the observation in Table 3.2 that the widely available vegetable oils operate up to a temperature of 453K, which may be a potential choice as a heat transfer fluid. Therefore, the vegetable oils are excluded at a higher temperature in Figure 3.5b at 573K. A careful investigation allows inferring the following:

a) Among all the pure fluids, Hitec-XL is preferred along with a higher FoM. It is also interesting to note that both the selected vegetable oils perform as well as the Hitec-XL at a temperature of 453K. One question remains regarding the stability of such an oil under thermal cycling and is of future interest. Experiments have demonstrated that such oils sustain up to 2160 hours of thermal cycling [15].
b) The vegetable oils outperform TherminolVP1/66, and Hitec-XL remained preferred among pure fluids at a temperature of 573K. Interestingly, TherminolVP1/66 is widely utilized for power generation with concentrated solar thermal systems using the parabolic trough collector. Moreover, solar salts are probably the next best option, being stable at a very high temperature of up to 873K.
c) The calculations show differences between computed FoM for nanofluids and hybrid nanofluids, such as CuO-CA and CuO-Al_2O_3-CA, and CuO-TVP1 and CuO-

Al_2O_3-TVP1, are 2-3%. Thus, some improvement is indeed expected using hybrid nanofluids.

d) Unfortunately, a similar analysis could not be performed with the Hitec-XL nanoparticle mixture due to the lack of a reliable Nu_{BF} for molten salt. Therefore, the current research activity refrains from venturing into the same using equation 3.4.

The analysis shows that FoM is more consistent than the dimensional parameters. One question remains whether this conclusion can be extended to a wider range of temperatures. To address this aspect, FoM is utilized to create look-up diagrams for a quick comparative assessment of the different heat transfer fluids. This is subsequently presented.

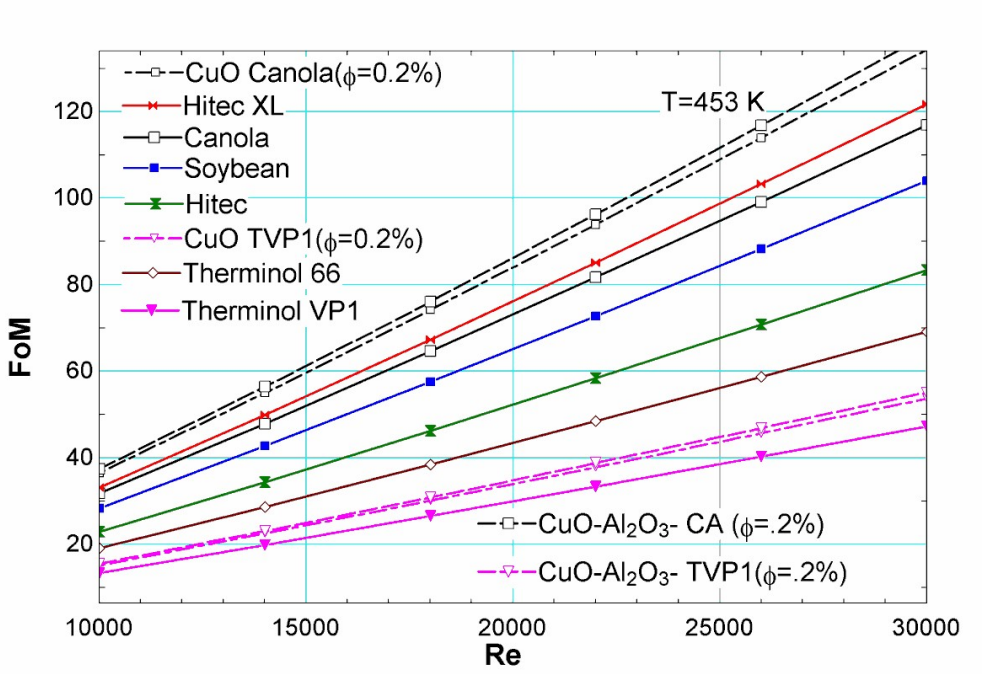

(a)

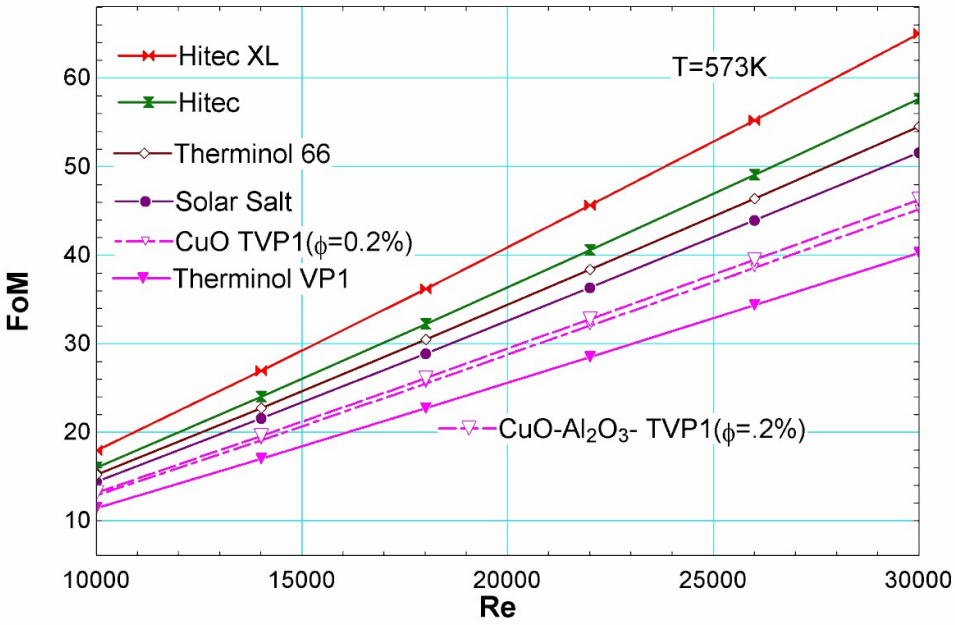

(b)

Figure 3.5 A comparative assessment of the non-dimensional figure of merit at (a) 453K and (b) 573K with different pure fluids, nanofluids, and hybrid nanofluids for φ = 0.2%.

3.2.4 Heat Transfer Fluid Selection: Look-up Diagrams

While investigating the dimensional and non-dimensional parameters, it is realized that a look-up diagram would be very helpful for selecting a heat transfer fluid with temperature-varying thermophysical properties. This is because all the above analyses are performed at a given temperature. However, the variation in fluid properties will alter their Prandtl number, which is not addressed. Therefore, the look-up diagram, as in Figure 3.6, is proposed. Nusselt number depends on the fluid and flow properties, represented by Prandtl (*Pr*) and Reynolds (*Re*) numbers. The coefficient of pressure (CP) is expressed in terms of *Re*. Thus, the non-dimensional FoM depends on *Re* and *Pr*. Therefore, a triangular-shaped qualitative diagram is created to represent FoM as f (Re, Pr). This provides a quick overview of the variation of FoM with *Re* and *Pr*. The dotted arrows indicate the direction of change and the range is a representative one. The range of *Re*, *Pr,* and FoM may be

altered depending on the applications and fluid in question. Here, the created diagram is based on thermophysical properties in 373-573 K.

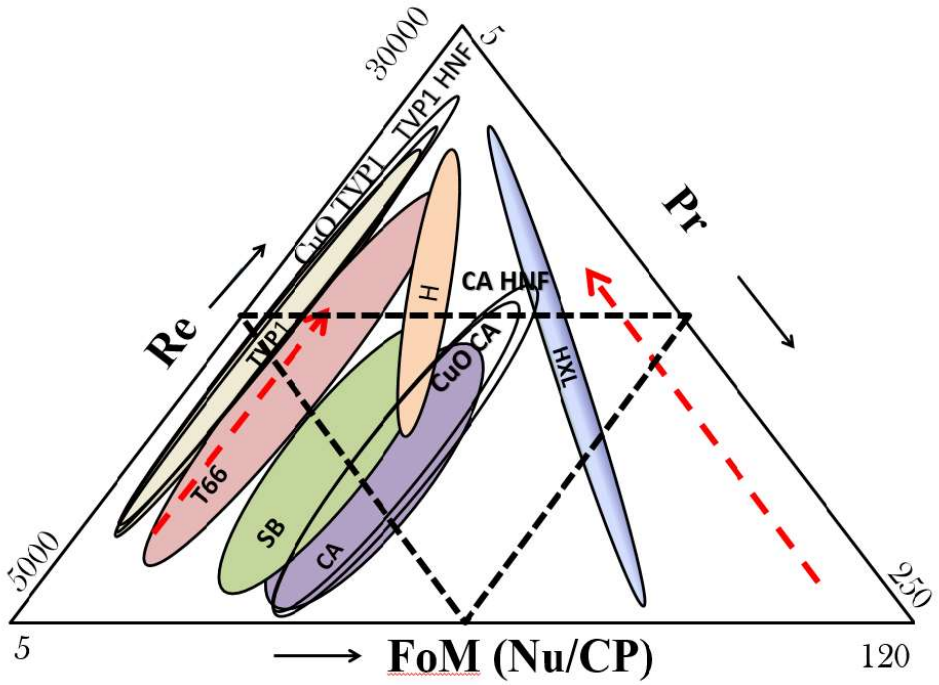

Figure 3.6 A qualitative look-up diagram for the selection of a heat transfer fluid, including nanofluids and hybrid nanofluids, for a temperature range of 373-573 K.

The qualitative diagram shows that for some fluid, the increasing *Re* and decreasing *Pr* leads to a high value of FoM. Whereas Hitec-XL (HXL) generally exhibits a high value of FoM, an increasing *Re* is suppressed by a relative decrease of *Pr*. Thus, FoM seems to decrease along the direction of the dotted arrow. A quick view of this diagram reveals that CuO-CAnano-oil and CuO-Al_2O_3-CA hybrid nano-oil may be equally preferred, up to an appropriate temperature, within the selected range. Furthermore, the increasing trend of FoM, for CuO-TVP1 nano-oil and CuO-Al_2O_3-TVP1 hybrid nano-oil with *Re,* allows concluding that these nano-oils may outperform HXL beyond a *Re*. Therefore, the qualitative look-up diagram helps in concluding that the turbulent flow of CuO-CA or CuO-

Al_2O_3-CA is preferable beyond a certain *Re* and *Pr*. Such conclusions, which can easily be drawn from a qualitative look-up diagram, demonstrate its advantage.

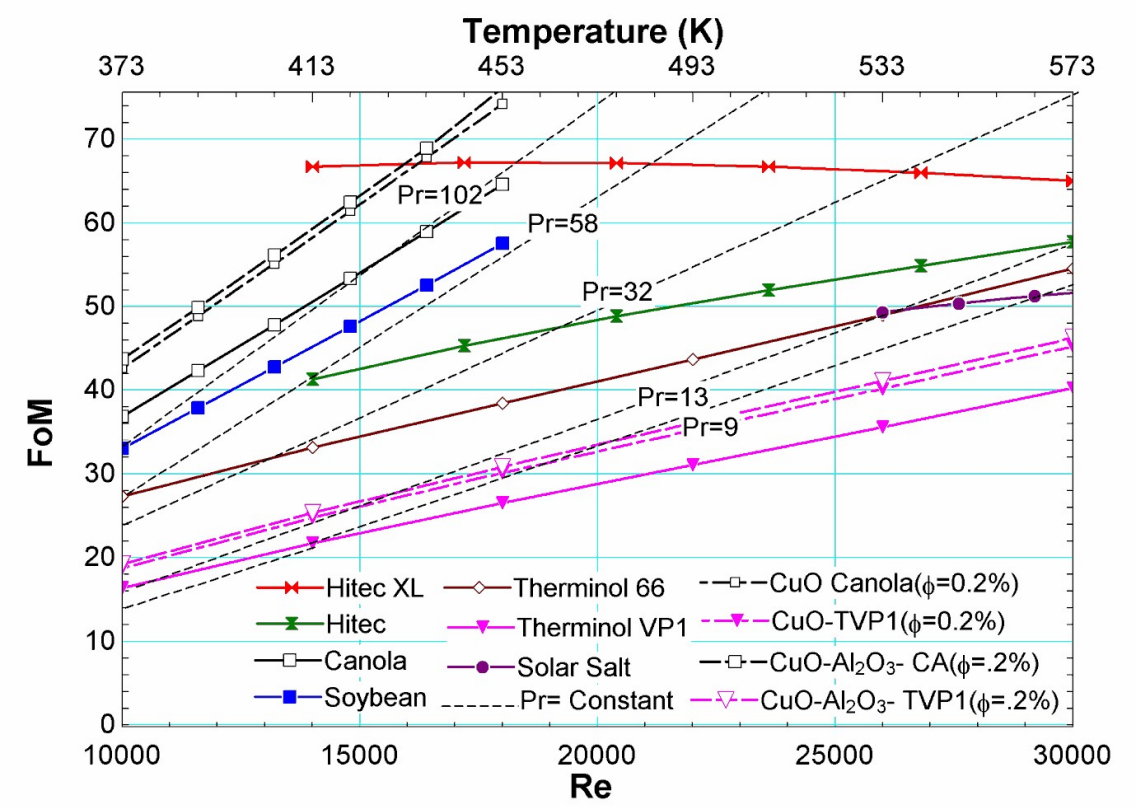

Figure 3.7 A Mollier-type quantitative look-up diagram for the selection of a heat transfer fluid.

The qualitative look-up diagram lacks quantitative information. Thus, a Mollier-type quantitative look-up diagram is created, and the same is represented in Figure 3.7. To draw this diagram, the operating temperature is regarded as an independent parameter, which is represented by vertically aligned isotherms. Subsequently, the computed values of FoM (*Nu*/CP) are indicated by varying the range of *Re*. All such points correspond to a particular temperature identified concerning the isotherms. Subsequently, the constant Prandtl number (*Pr*) lines are drawn based on the temperature-dependent fluid properties.

Thus, the quantitative look-up diagram provides in one shot the entire gambit of the relationship between the FoM and the relevant parameters. It should be noted that the constant *Pr* lines represent a certain ratio of viscous to thermal boundary layer thickness. This is also important for analyzing the penetration of heat into the fluid layers and flow resistance owing to shear stress on the wall.

A close inspection of this diagram reveals that HXL remains the most preferred until 453K, and vegetable oil, if found, maybe a better choice for pure fluid at a temperature > 453K. Qualitative analysis reveals that CuO-CA nano-oil or CuO-Al_2O_3-CA hybrid nano-oil should be preferred beyond 423K. This is attributed to the enhanced heat transfer properties of CA with the suspended nanoparticles and is evident along the constant *Pr* line. The same is true for CuO-Al_2O_3-TVP1 hybrid nano-oil in comparison to TVP1. The calculation shows an increase of FoM by about 10-30 % for CA or TVP1-based nano-oils in comparison to the base fluid (CA or TVP1). Thus, it is concluded that (a) the use of CuO-TVP1 or CNT-TVP1 or hybrid nano-synthetic-oils will be beneficial for parabolic trough-based power plants, (b) CuO-CA/ CuO-Al_2O_3–CA or such a hybrid nano-(vegetable)oil should be investigated for an application in the temperature range 373-573 K. The quantitative diagram reveals that the *Pr* of HXL salt decreases substantially with increasing temperature. This leads to its reduction in heat transfer capability, which is discussed using the qualitative look-up diagram in Figure 3.6. Finally, analysis shows that FoM will remain within ± 10%, satisfying the uncertainty range, for a change of c_p by ±60%, which is perhaps an extreme case. This accounts for the uncertainty of this important parameter, to a certain extent, on FoM for practical applications. Thus, the qualitative and quantitative diagrams are likely to help select a heat transfer fluid.

3.2.5 Heat Transfer Fluid: Cost-benefit Analysis

A preliminary comparative cost-benefit analysis is performed for nanofluids. This is summarized in Table 3.8, which reveals that (a) the cost of vegetable oil is lower than that of widely used Therminol by 3-4 times, (b) vegetable oils are locally available and are generally non-toxic, (c) the cost of solar salts is comparable to that of vegetable oil, however, not readily available, (d) solar salt is not so corrosive for Cu, (e) Therminol is very corrosive for Cu and (f) detailed investigations are required for corrosive nature of vegetable oil/vegetable nano-oil. Thus, the analysis allows the conclusion that vegetable oil will certainly be beneficial in terms of heat transfer capability and cost-wise for practical systems.

Table 3.8 Cost of heat transfer fluids and their benefit for practical applications [117].

Heat transfer fluid	Flashpoint (K)	Cost ($/kg)	Toxic	Corrosive
Canola Oil	600	0.70	No	-
Soybean Oil	600	0.57		-
TherminolVP1	383	2.10	Yes	High (for Cu)
Therminol 66	448	2.10		
Hitec XL	Non-flammable	1.19		Low (for Cu)
Hitec	Non-flammable	0.93		
Solar salt	Non-flammable	0.49		

3.3 Summary

This chapter deals with the selection of heat transfer fluids for solar thermal system-based heating and cooling applications in the range of 373-573 K. The fluids include pure fluid and nanofluids, which are either utilized or have shown some potential as heat transport media. The following are the major findings of this chapter:

a) An analysis of dimensional parameters using the thermophysical properties of pure and nanofluid reveals that the relative performance of a heat transfer fluid depends on the temperature and rather changes with the same. Thus, a non-dimensional figure of merit (FoM = *Nu*/CP) is proposed to analyze the heat transfer with a fluid relative to the offered pressure drop. A high value of FoM is preferred for a heat transfer fluid.

b) To estimate FoM for nanofluids, the following improved Nusselt number correlation (Nu_{NF}) is proposed based on an extensive analysis of experimental data:

$$Nu_{NF} = 0.074 {Re_{NF}}^{0.72} {Pr_{NF}}^{0.22} \text{ with } 10000 < Re_{NF} < 25000.$$

This correlation predicts experiments with CuO-water, TiO_2-water, Cu-water, and CNT-water, mostly, within ±20% except for Graphene nanoplatelet.

c) Finally, using a separation approach, the following generalized form of Nusselt number correlation for nanofluids is obtained:

$$\underbrace{Nu_{NF}}_{\textbf{experimental}} = \underbrace{0.93\ {\alpha_r}^{-0.059} \phi^{-0.026} n^{0.357}}_{\textbf{correction factor } (\eta)} \underbrace{\left\{ \frac{\frac{f}{8}(Re - 1000)Pr}{1 + 12.7\sqrt{\frac{f}{8}}\left(Pr^{\frac{2}{3}} - 1\right)} \right\}}_{\textbf{Gnielinski correlation, } Nu_{BF}}$$

This correlation filters out the effect of nanoparticles for a known *Nu* for the base fluid (Nu_{BF}). Thus, the representation benefits from the fact that (i) the Gnielinski

correlation for Nu_{BF} is valid for vegetable oil, therminolVP1 with 0.5<Pr<2000, and (ii) the correction factor (η) describing the effect of the nanoparticle is based on a wide range of thermophysical properties, shapes, and sizes. This correlation is utilized for estimating FoM in which Therminol and vegetable oils are used as base fluid in the 373-573 K temperature range. The correlation for Nu_{NF} makes use of a model for c_p that excludes the effect of internal and nanoscopic organization of the nanofluid/nanosalt, which becomes a limitation for this correlation as well.

d) Finally, realizing the limitations of dimensional parameters and their representations, qualitative and Mollier-type quantitative look-up diagrams are created. A comparative assessment shows that FoM, for CuO-Canola/TherminolVP1 nano-oil or CuO-Al_2O_3-Canola/TherminolVP1 hybrid nano-oil, increases by about 10-30%, in comparison to Canola or TherminolVP1 oil. Therefore, Canola-oil, CuO-canola nano-oil, or CuO-Al2O3-Canolahybrid nano-oil are suggested for the 373-473 K temperature range with FoM value comparable to Hitec-XL salt. Furthermore, the use of TherminolVP1-based nano-oil or hybrid nano-oil will be beneficial for parabolic trough collector-based concentrated solar thermal power generation systems.

e) The two important questions to be answered for oil-based nanofluids are (a) the stability, (b) the uncertainty of deduced Nu_{NF}, and (c) corrosion. These require dedicated experiments and are foreseen in the future.